Vol. 83 No. 6 pp. 1031–1040 ACTA GEOLOGICA SINICA (English Edition) Dec. 2009

Structure, Orientation and Finite Element Analysis of the Tail Club of *Mamenchisaurus hochuanensis*

XING Lida[1, *], YE Yong[2], SHU Chunkang[2], PENG Guangzhao[2] and YOU Hailu[1]

1 *Institute of Geology, Chinese Academy of Geological Sciences, Beijing 100037, P. R. China*
2 *Zigong Dinosaur Museum, Zigong, Sichuan Province 643013, P. R. China*

Abstract: The structure and orientation of the posterior extremity (tail club) of the caudal vertebrae of *Mamenchisaurus hochuanensis* Young and Chao, 1972 from the Upper Jurassic Shangshaximiao Formation has been analyzed to determine the tail club function using Finite Element Analysis. Of the four caudal vertebrae composing the tail club, the second largest (C"1") was probably the most proximal, and is fixed with the preceding sequence of the caudal vertebrae, whereas the smallest (C"4") is free and forms the termination of the tail club. Our analysis also suggests that the tail club is more efficient in lateral swinging rather than up-and-down motion, and that the best region for the tail club to impact is at the spine of the largest of the four caudals (C"2"), with a maximum load for impact at about 450 N. The tail club of *Mamenchisaurus hochuanensis* probably also had limitations as a defense weapon and was more possibly a sensory organ to improve nerve conduction velocity to enhance the capacity for sensory perception of its surroundings.

Key words: *Mamenchisaurus*, tail club, Finite Element Analysis, Shangshaximiao Formation, Jurassic

1 Introduction

Mamenchisaurus is a sauropod dinosaur discovered mainly from the Middle–Late Jurassic of China. *Mamenchisaurus constructus,* the type species, was described by Young (1954) based on an incomplete specimen. Since then, several more species have been established, including *M. hochuanensis* (Young and Chao, 1972), *M. youngi* (Pi et al., 1996), *M. anyuensis* (He et al., 1996), *M. jingyanensis* (Zhang et al., 1998), *M. sinocanadorum* (Russell and Zheng, 1993), *M. yunnanensis* (Fang et al., 2004) and two suspect or invalid taxa, "*M. fuxiensis*" (*Zigongosaurus fuxiensis*, Hou et al., 1976; nomen nudum see Li and Cai, 1997) and "*M. guanyuanensis*" (nomen nudum see Li and Cai, 1997). Although a reasonable amount of material for *Mamenchisaurus* has been collected, much is incomplete, and especially the tail end is often missing, and therefore, the presence of a tail club in the genus was uncertain until 2001 (see below). In contrast, a tail club was confirmed to be present in *Shunosaurus* (Zhang et al., 1984) and *Omeisaurus* (Dong et al., 1989) from the Sichuan Basin, where a number of species of *Mamenchisaurus* (including the type) are known as well.

In 1995, a nearly complete skeleton (ZDM 0126) of *Mamenchisaurus hochuanensis* was collected from the Upper Jurassic Shangshaximiao Formation, near Zigong City (Ye et al. 2001). Most of ZDM 0126 is preserved in articulation, including some sections of the vertebral column and the discovery revealed the terminal caudal vertebrae of *Mamenchisaurus* for the first time. The four posteriormost caudal vertebrae of ZDM 0126 are enlarged and fused into a tail club, with a coronal shape, which is significantly distinct from the hammer-like tail clubs of *Shunosaurus* and *Omeisaurus.* Although there are 45 caudal vertebrae preserved in ZDM 0126, only the proximal 26 vertebrae are associated in sequence. The tail club is preserved at the distal extremity but because it is disarticulated from the rest of the caudals, the orientation is uncertain. The two ends of the club are dissimilar in size; one end is larger than the other. Ye et al. (2001) assumed that the caudal vertebrae were arranged in the sequence from small to large. In 2002, Ouyang and Ye thought that the opposite was true and further considered that the coronal-tail club of ZDM 0126 is equivalent to the caudal vertebrae anterior to the tail club in *Shunosaurus* (ZDM 2006) and argued that there was a hammer-like club articulated with the coronal-tail club.

* Corresponding author. E-mail: xinglida@gmail.com

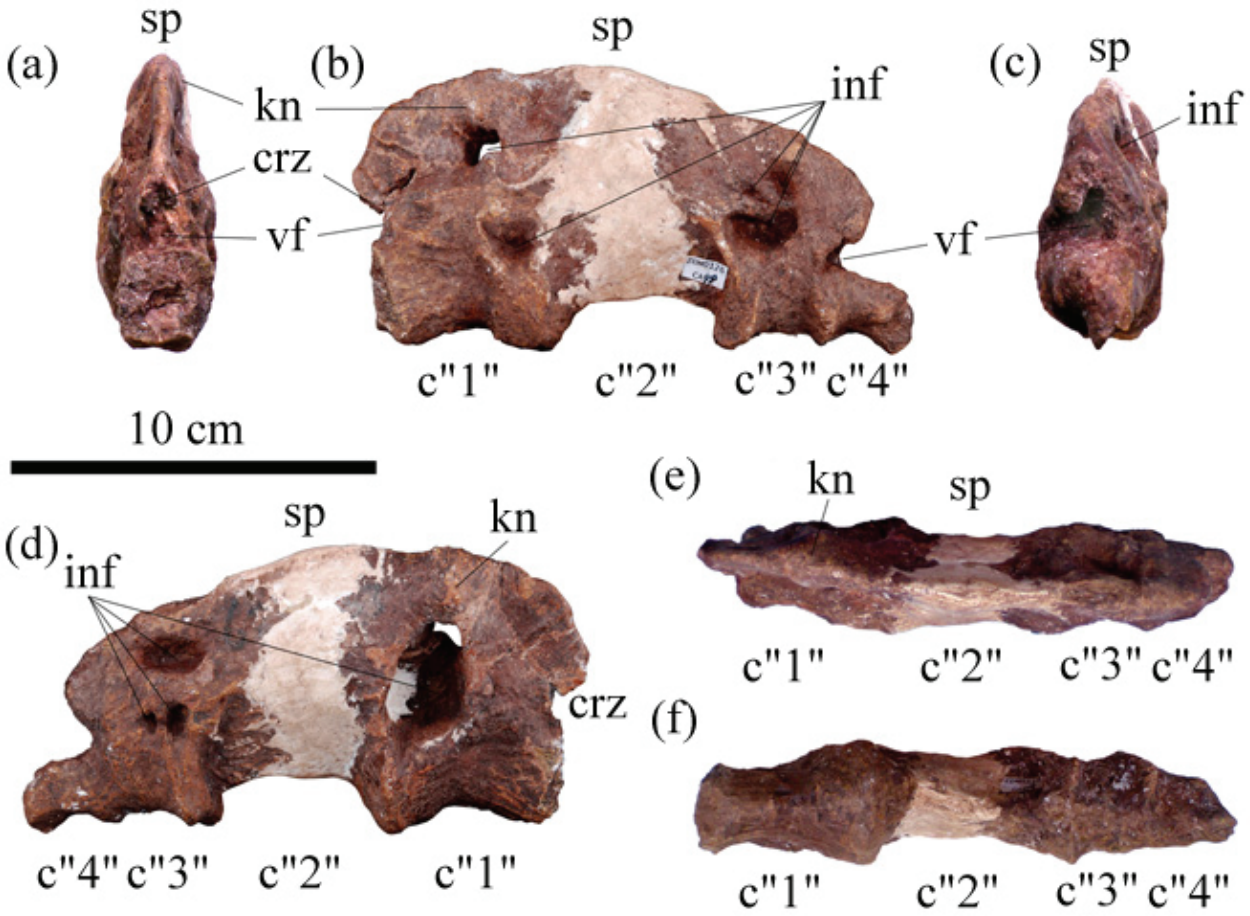

Fig. 1. Tail club of *Mamenchisaurus hochuanensis* ZDM 0126.
(a), cranial, (b), left lateral, (c), caudal, (d), right lateral, (e), dorsal, and (f), ventral views. Scale bar represents 10 cm. Anatomical abbreviations: crz, cranial zygapophysis; inf, intervertabral fossa; kn, knob; sp, spine; vf, exit/opening of vertebral/neural canal.

2 Materials and Methods

2.1 Structure and orientation of tail club of *M. hochuanensis* ZDM 0126

The tail club of ZDM 0126 is fused from four caudal vertebrae, C"1" to "4" proximo-distally (Fig. 1). It is 156.5 mm in length (see Table 1 for the length of each vertebra). C"1"–C"3" are completely preserved; the C"4" has the centrum preserved only, with the neural arch and spine missing. In ventral view, there are three fused sutural lines between these four caudal vertebrae. The fused suture is weakly crest-like. The C"1" centrum gradually enlarges proximo-distally and there is a concave articular surface at the proximal end. The C"2" centrum is the longest, its diameter gradually reducing proximo-distally. The C"3" centrum is short and distinctly constricted, merely 38% of the length of C"2". The C"4" centrum is the shortest, being slightly shorter than C"3", with no distinct articular facet at the caudal end. The lateral surface of the tail club is wide and flat, and distinctively concave in some areas. A neural arch is developed. A weak cranial zygapophysis is preserved at C"1". The spine reaches the highest point where C"1" and C"2" are fused, and then gradually decreases in height towards the posterior end. The

Table 1 Selected measurements of the tail club of *Mamenchisaurus hochuanensis* (ZDM 0126)

Cd No.	Lc	Anh	Anw	Poh	Pow	Arl	Sph	Dpw	Nch	Ncw
'1'	48	32.1	27.6	-	-	36.3	55.1	16.1	3.1	4.9
'2'	61.2	33	37.1	-	-	62.2	42	15	9.3	11.2
'3'	23.8	31.9	31.2	-	-	25.8	34.5	19.9	12.1	12.8
'4'	23.5	23.2	25.8	12	9.5	-	-	-	-	-

Abbreviations: **Anh**, height of centrum on its anterior surface; **Anw**, width of centrum on its anterior surface; **Arl**, length of the arch on the dorsa surface of the centrum; **Cd**, caudal vertebra; **Dpw**, transverse width of the spine crest across its posterior surface; **Lc**, length of centrum; **Nch**, height o neural canal; **Ncw**, width of neural canal; **Poh**, height of centrum on its posterior surface; **Pow**, width of centrum on its posterior surface; **Sph**, height o spine. Measurements are in mm.

vertebral/neural canal gradually becomes wider distally, and its terminal exit is an inverted U-shape and opens at the caudal end of C"3". The terminal foramen of the vertebral/neural canal is four times as wide as that in C"1".

Shunosaurus lii (ZDM 5006) is a juvenile individual. The end of its caudal vertebrae is terminated directly by a tail club (Zhang et al., 1984 and Peng et al., 2005), whereas the tail clubs in ZDM 5013, ZDM 5035, ZDM 5045, ZDM 5046, ZDM 5047, ZDM 5051 and ZDM I-M are all isolated, disarticulated from the caudal vertebrae. The shapes of these tail clubs are different, and they might belong to two or three different sauropod taxa; nevertheless, they share the following common features; the tail club is spindle shaped and the vertebral/neural opening enlarges at the distal end. Although the tail club of ZDM 0126 is not spindle shaped, the vertebral/neural foramen of the neural canal enlarges in the same way as in the aforementioned clubs. The tail club of ZDM 5045, which is the most complete one of all, consists of five fused caudal vertebrae. The central lengths of the five caudals are 50.8 mm, 58.2 mm, 72.6 mm, 33.4 mm and 37.1 mm in proximo-distal sequence. Compared with the tail club of ZDM 5045, that of ZDM 0126 might have also been formed by five caudals. Although no data is available for ontogenetic variation in the tail club of *M. hochuanensis*, we think that the involved caudals might have first become larger distally and then smaller towards the end, with the last two vertebrae being the smallest in this sauropod.

2.2 Finite Element Analysis of the Tail Club of *M. hochuanensis* ZDM 0126

Finite Element Analysis (FEA) is a technique that reconstructs stress, strain, and deformation in a digital structure. Although widely used in engineering and orthopedic science for more than 30 years, it has only recently been adopted to paleontology in investigating the skeletal behavior of fossil vertebrates (Jenkins, 1997; Rayfield, 1998; Rayfield et al., 2001; Fastnacht et al., 2002; Jenkins et al., 2002; Snively and Russell, 2002). Visualizing skeletal stress and strain in motion provides an insight into skeletal design and optimization, and the Finite Element Method (FEM) can offer such an opportunity (Thomason, 1995). Recently, FEA has been often used in mechanical analysis of the skulls of theropods (Rayfield, 1998, 2004, 2005a,b, 2007; Rayfield et al., 2001, 2002; Boyd, 2007), sauropods (Witzel and Preuschoft, 2005) and an ornithopod (Laura, 2007) and dinosaur tracks (Falkingham et al., 2007).

2.2.1 Results of Three-Dimensional Model

The construction of the Finite Element Model of the tail club of *M. hochuanensis* ZDM 0126 requires its three-dimensional (3D) geometric data (Fig. 2). We adopted the entity scan method, i.e. scanning the fossil of the tail club to obtain the 3D data, and later reconstructed the 3D model of the fossil in a computer. The machine we employed is a Non-contact Grating-Type Structured Light 3D Scanning Systems (JiRui II, see Table 2) made in China (made in Beijing JiRui Xintian Technology Co. Ltd). High precision, which is adept at reconstructing complex structures was used during the course of the scan. After the high-precision 3D data of the tail club of ZDM 0126 was obtained, it was saved as IGES (The Initial Graphics Exchange Specification) files in computer-aided design (CAD) systems.

Table 2 JiRui II 3D Scanning Technical Data

Type	JRXS (explain)
Unit scan scope (mm^2)	150×100–200×150
Precision of measurement (mm)	0.01–0.02
Unit measurement points	About 1,330,000 points
Average pixel pitch (mm)	0.1–0.15
Scan speed for single surface	<10S
Connection manner	Automatically connected

Abbreviations: JRXS = Beijing JiRui Xintian Technology Co. Ltd

Currently, the common finite element analysis softwares are ANSYS, MARC, ABAQUS, and MSC. Patran/Nastran. MSC. Patran/Nastran was selected for this experiment because it is the leading pre- and post processor and the MSC. Nastran. The software is a compositive parallel-framed finite-element pre- and post processor and analysis-simulation system.

2.2.2 Division of Mesh and Parameters of Materials

We took the tail club of *M. hochuanensis* ZDM 0126 into dispersion first. On meshing, 5258 ten-node solid tetrahedral elements were produced, comprising 8649 nodes with 51894 degrees of freedom (Fig. 3). Elements were ascribed the material properties of bovine Haversian bone, on the basis of similar histological structure in theropod and bovine bone; they are: Young's modulus=10 GPa; Shear modulus=3.6 GPa; Poisson ratio, 0.4; density, 1.895 kg/m^3 (Rayfield et al., 2001). There are often various choices for the selection of the parameters of materials whereas the distribution of the stress of the tail club is determined by the load. The effect of the parameters on the materials is weak. The change of the parameters of the materials mainly affects the deformation of the vertebrae.

Regarding maximum load and allowable stress, such loads are defined here as the maximum load the tail club structure could withstand before stresses or strains in the model reached a point where in life, bony tissue would begin to yield plastic non-recoverable deformation. This value was taken as 200 MPa (Rayfield et al., 2001;

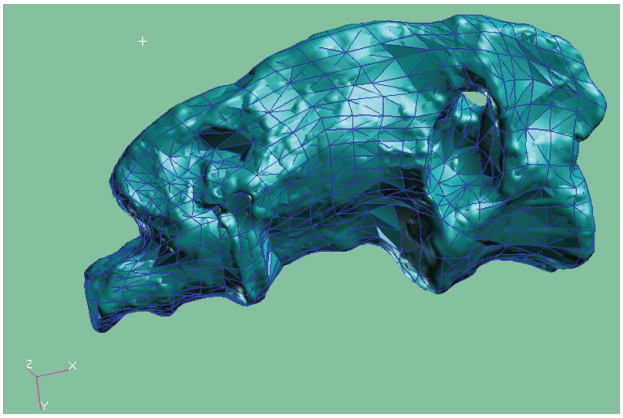

Fig. 2. A geometric three-dimensional model of the *tail club* of ZDM 0126.

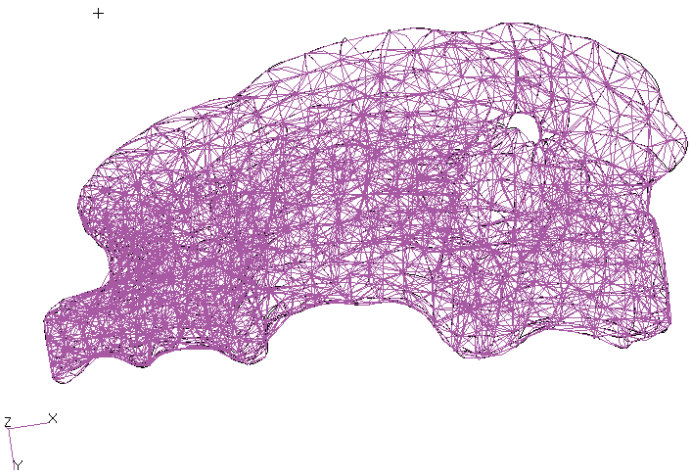

Fig. 3. The mesh construction of the tail club of ZDM 0126.

Rayfield, 2005b).

2.2.3 Modal Analysis

We adopted the Lanczos method (Komzsik, 2003) to evaluate the eigenvalue of the tail club in the experiment. The Lanczos method is a new method for the solution of eigenvalue, which combines the tracking method and changes; it is very efficient for the evaluation of eigenvalues of sparse matrix where a great amount of calculation is involved. We submitted the data to MSC. Nastran for calculation and the inherent frequencies of the tail club came out. Selecting the frequencies of the first four order modes, of which the frequencies in the first order through to fourth order modes are 2237.9, 2972.1, 3624.1 and 4930.1 in sequence, we analyzed the distribution of the corresponding modal displacement of the order mode. See the nephogram below (Fig. 4).

We can draw the conclusion from the modal analysis

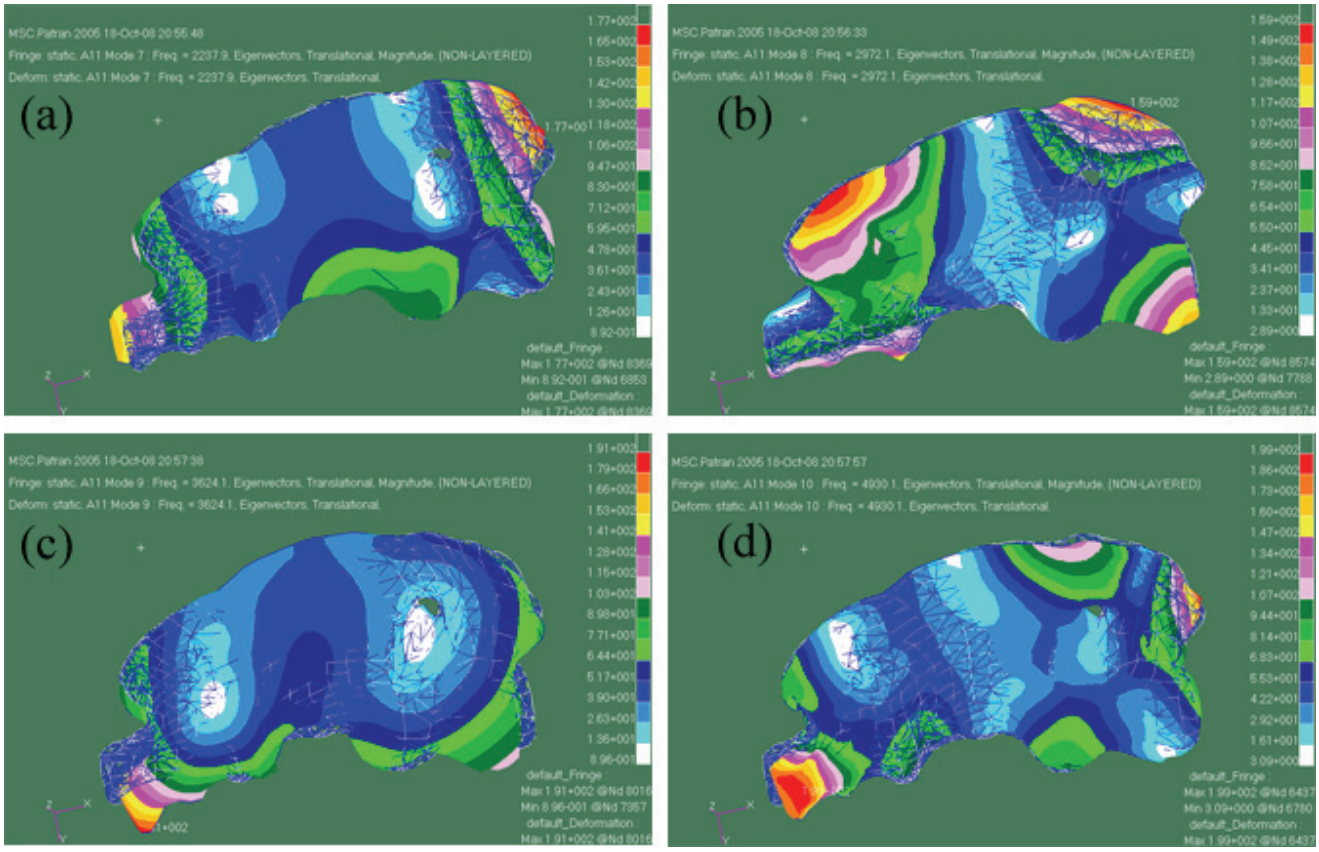

Fig. 4. Nephogram for modal displacement of inherent frequencies of four order modes of the tail club: (a), First order mode; (b), Second order mode; (c), Third order mode; (d), Fourth order mode.

that the average modal displacement of the caudal side is greater than that of the cranial side whereas the stiffness of the cranial side is greater than that of the caudal side, which meets the actual situation in general. The stiffness is contributed by the larger cross section of the cranial side, which possesses more materials, and i.a. had more energy savings.

Furthermore, as indicated in Fig. 4(a-d), we can conclude that the basic modal displacement, which belongs to the lowest region of the color blocks, is relatively tiny and located at the middle of the tail club, especially seen in the spine region of C"2". It is the commonly the strongest region of stiffness for the (a)-(d) modal, being suitable for impact.

2.2.4 Load Case Analysis

The purpose of this study is to analyze the distribution of the stress in different cases, and to compare the value of the failure load corresponding to any certain case for the determination of the mechanical properties of the tail club.

Case A. The caudal side was clamped. The cranial side was loaded (i.e., subjected to tension) (Fig. 5). When the maximum stress reached the value of allowable stress, the load of the cranial side was 180N. In this case, when the load is over 180N, the stress on the tail club is overexerting and causes failure.

Case B. The cranial side was clamped. The caudal side was loaded (subjected to tension) (Fig. 6). When the maximum stress reached the value of allowable stress, the load of caudal side was 200N. In this case, when the load is over 200N, the stress on the tail club is overexerting and causes failure.

Case C. The cranial side was clamped. The caudal side was loaded (subjected to lateral force). We observed that the region of the stress is small and concentrated at the clamped end of the cranial side (Fig. 7). The concentration of the stress is due to the restriction and can be ignored. The 5th deep blue strip (marked by the red arrow) on the right side of the figure is the region of maximum stress, with the exception of the stress concentration region. When the stress reached the allowable value, the load of the caudal side was 65N. In this case, when the load is over 65N, the stress on the tail club is overexerting and causes failure.

Case D. The caudal side was clamped. The cranial side was loaded (subjected to lateral force) (Fig. 8). The concentration of the stress is due to the restriction and can be ignored. The deep blue strip (marked by the red arrow) is the region of maximum stress, with the exception of the stress concentration region. When the stress reached the value of the allowable stress, the load of cranial side was 20N. In this case, when the load is over 20N, the stress on the tail club is overexerting and causes failure.

Case E. The value and boundary condition are the same as those of Case C. We changed the load form Y-axis direction singly. Comparing the situation seen in Figure 9 with that of Figure 7, we see that under the same load, the average stress is much less in Case E than C.

The following conclusions can be drawn from Cases A-E: (1) both the strength and the stiffness are stronger on the cranial side than on the caudal side; (2) no significant difference in load is recognized between the two terminals (x-axis direction, tension) and therefore, it is difficult to determine which side is fixed by the load of the x-axis direction because the differentiation is not large enough; (3) the difference in load between the two transverse terminals (z-axis direction, lateral force) is significant, being treble and above. Such a differentiation can provide reliable evidence for the determination. Therefore, the result of the simulation FEA supports the conclusion that C"1" was on the cranial side of the tail club, and C"4" was on the caudal side.

Case E further indicates that the left-right swing of the tail club would have been more efficient than swinging up and down. When the tail club swung from left to right, where the animal was subjected to a considerable lateral force, the stress of other regions was much lower (Figs. 7, 8), with the exception of the stress on the cranial side of the tail club, which was concentrated by the articulation with the caudal vertebrae (this phenomena should have been less serious in life).

From the abovementioned modal analysis, we know that the spine region of C"2" is the most suitable region for impact. We can get the initial stress-distribution diagram by enforcing a certain amount of load on the region and submitting the data to MSC. Nastran for calculation to determine if the load is enough. If not, we return to redefine the value of the load. Repeating the course of enforcing the load until it approaches the allowable stress (Fig. 10). The deep blue region is the maximum stress with the exception of the stress-concentration region on the cranial side of the tail club. When the stress reaches the allowable value, the load is at the maximum of around 450 N.

3 Discussion

We have determined the orientation of the tail club of *M. hochuanensis* in ZDM 0126 and discussed the suitable direction for swing, and the maximum impact load for the best point using FEA. These data make possible further discussion for the functions of the tail club.

Articulated terminal ends of the caudal vertebrae are rare in sauropod dinosaurs. In recent times, the ‘whiplash’

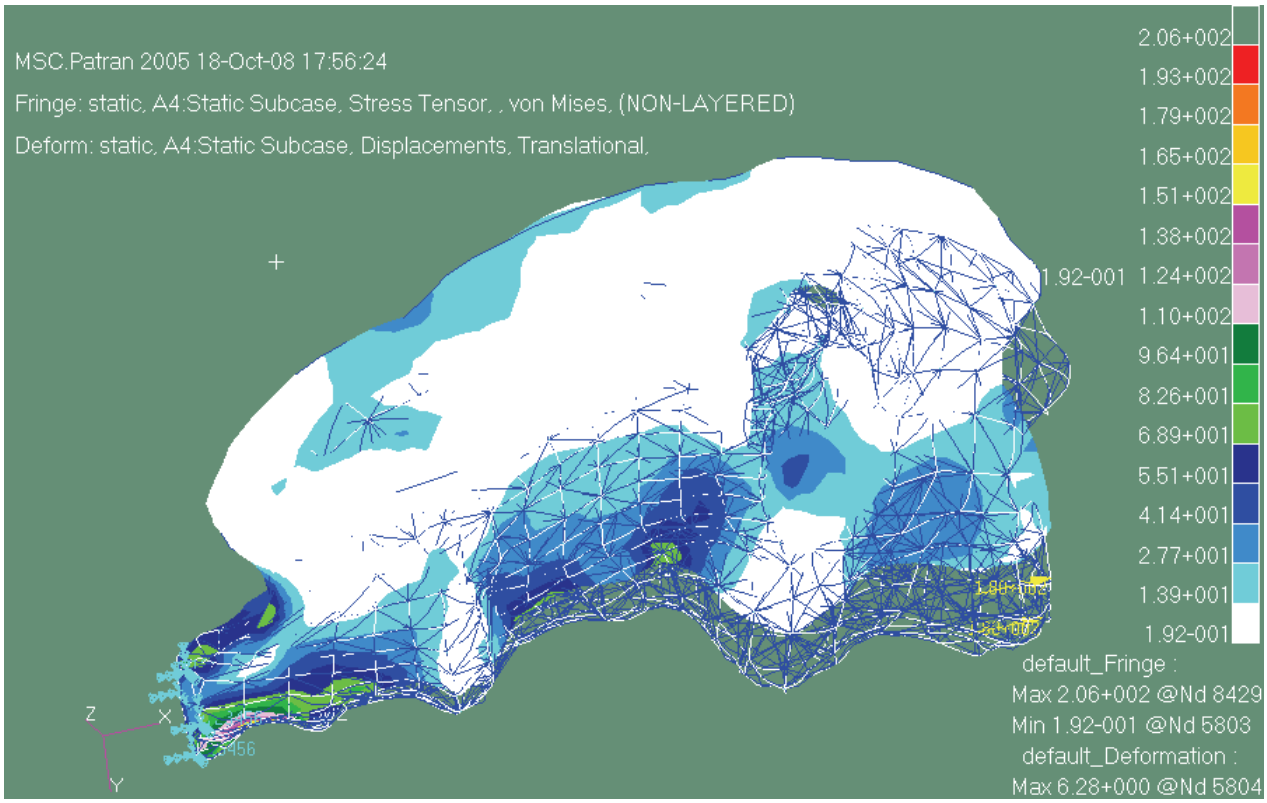

Fig. 5. The Von Mises stress of Case A.

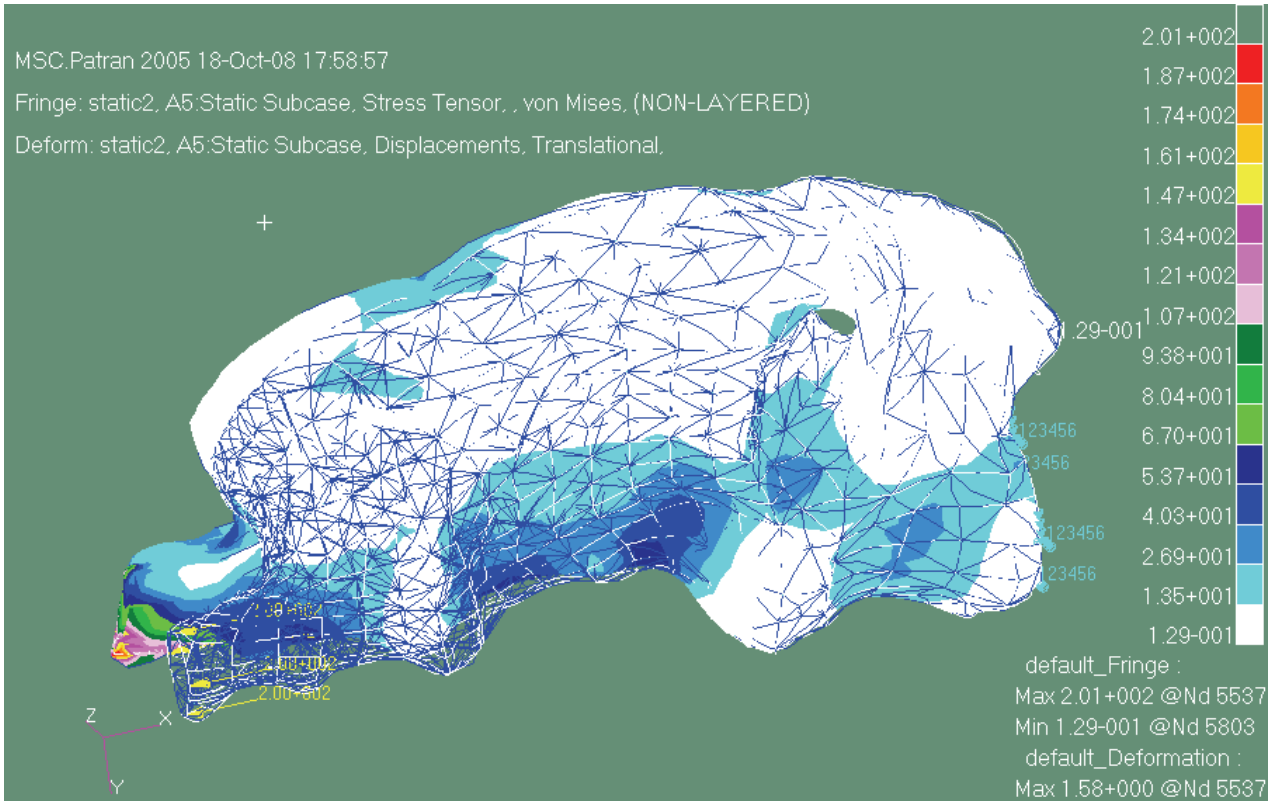

Fig. 6. The Von Mises stress of Case B.

tail (Gilmore, 1936; Holland, 1906) of the diplodocids *Apatosaurus* and *Diplodocus*, the hammer-like tail club (Zhang et al., 1984; Dong et al., 1989) of *Shunosaurus lii*, the coronal tail club (Ye et al., 2001) of *Mamenchisaurus hochuanensis*, the smooth terminal caudal vertebrae *of Gobititan shenzhouensis* (You et al., 2003), and the

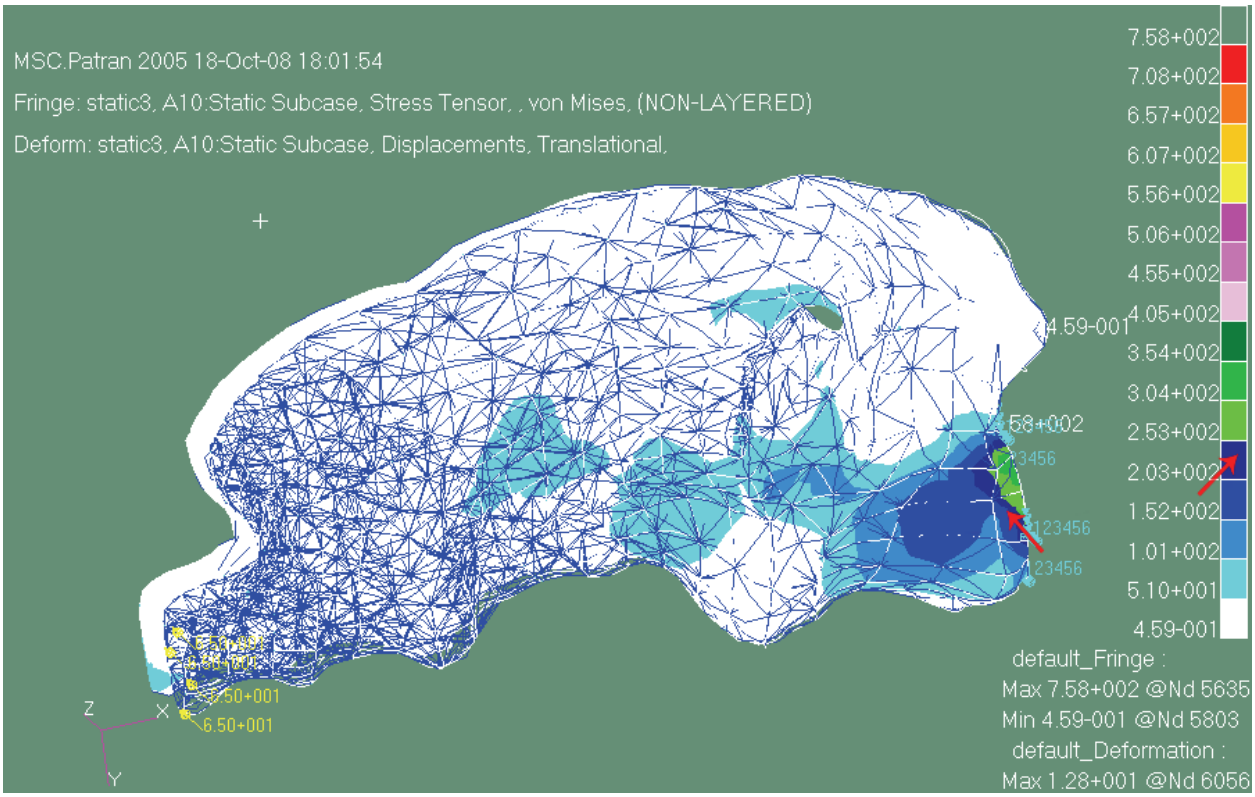

Fig. 7. The Von Mises stress of Case C.

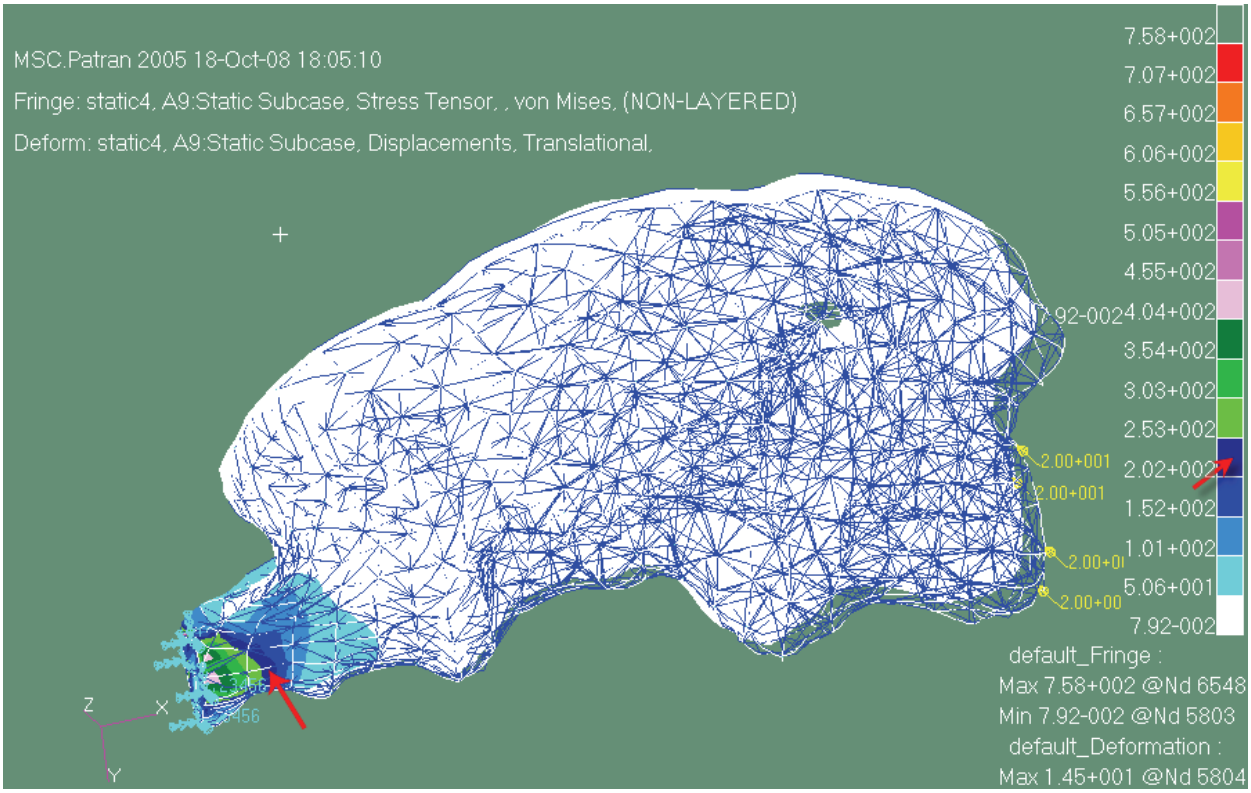

Fig. 8. The Von Mises stress of Case D.

biconvex caudal vertebrae (Wilson et al., 1999) of a titanosaur have all been discovered.

Diplodocids had an extremely long tail. The 82 caudal vertebrae (Holland, 1915) are much greater than the 44 caudal vertebrae (Peng et al., 2005) of *S. lii* (ZDM 5006) and the 50 or so caudal vertebrae (Ye et al., 2001) of *M.*

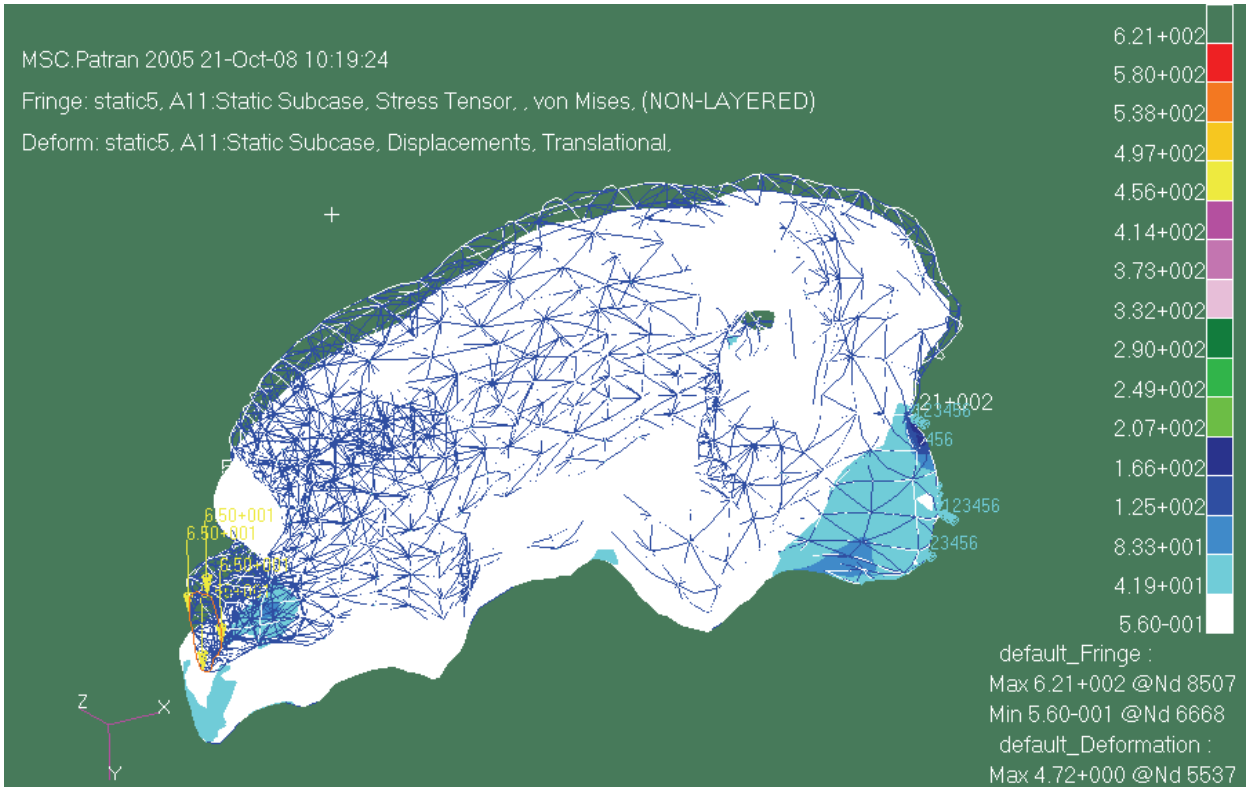

Fig. 9. The Von Mises stress of Case E.

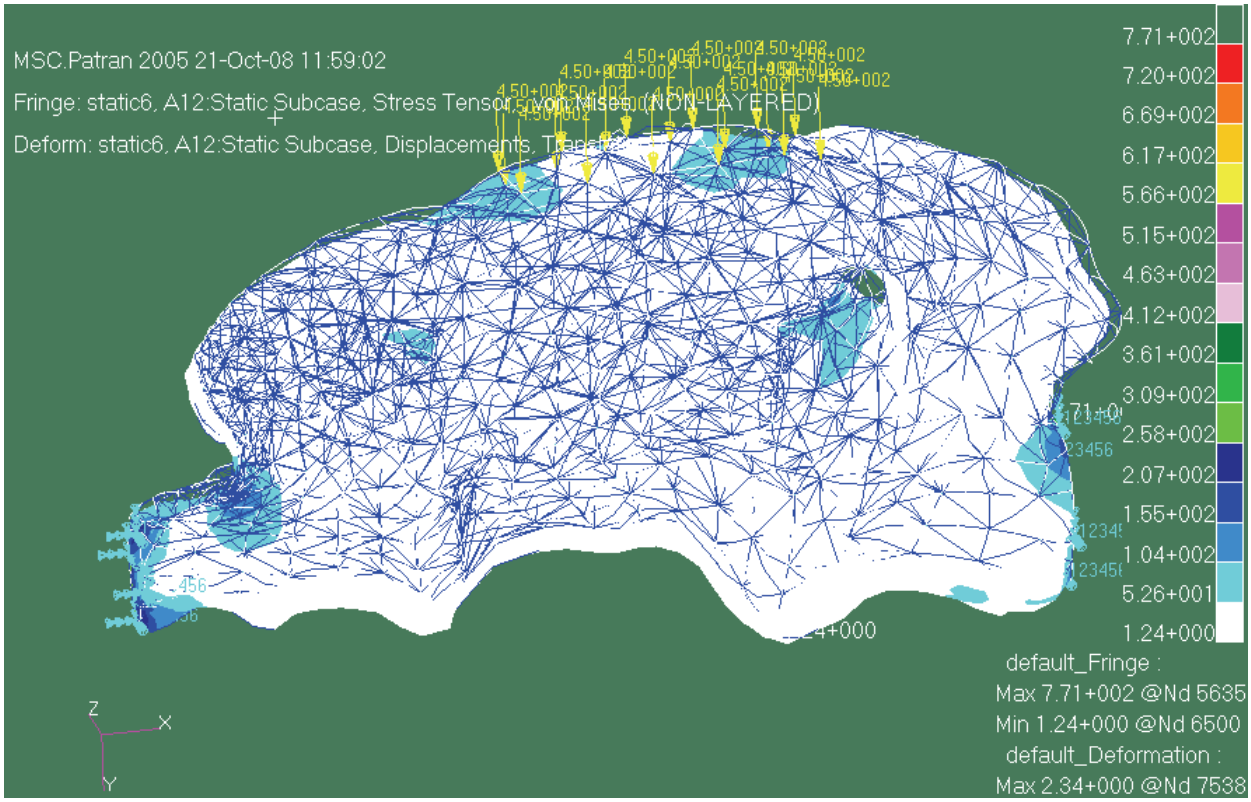

Fig. 10. Loads enforced on the spine region of C"2".

hochuanensis (ZDM 0126). Myhrvold and Currie (1997) noted that the whiplash tail "was not well adapted as a direct-impact weapon". They suggested using computer modeling that the tail-tip could be moved at 540 m/s, fast enough to generate a supersonic impact. This impact was most possibly for defense, communication, intraspecific

rivalry or courtship. In contrast, the tail of *S. lii* and *M. hochuanensis* is shorter, the sequential proportion of tail club to caudal vertebrae is not high (less than those of most ankylosaurs), and the texture is not very hard. The coronal tail club of *M. hochuanensis* is thinner than the hammer tail club of *S. lii*.

In addition, both *S. lii* and *M. hochuanensis* lack some key structures of ankylosaur tails. For example, the centra of the distal half of the caudal series are fused together, forming a rigid "handle" of vertebrae (Vickaryous et al., 2004) *in Ankylosaurus* (AMNH 5214) (Coombs, 1978) and *Euoplocephalus* (AMNH 5245, ROM 784 and ROM 788) (Coombs, 1995). Due to the absence of ossified tendons, *M. hochuanensis*, even *S. lii,* could not have forcefully whipped the tail club. Overexersion would have caused injury at the articulation between the tail club and the terminal caudal vertebrae.

Enlargement of the neural canal is present both in *S. lii* and isolated tail clubs (Dong et al., 1989) and also in *M. hochuanensis*, whereas this enlargement is not present in the terminal caudal vertebrae of other dinosaurs. Interestingly, it is present in the sacral plexus of stegosaurs but the function of such an enlargement is not definitely known but it was postulated to facilitate the supply of glycogen to the animal's nervous system (Buchholz, 1990). However, this is not applicable to *S. lii* and *M. hochuanensis* because the sacral plexus of stegosaurs is many times greater than its possible brain volume (Galton and Upchurch, 2004), whereas the neural canal of *S. lii* and *M. hochuanensis* has no such development. The enlargement of the neural canal of the tail club in *M. hochuanensis* might have favored improvement of Nerve Conduction Velocity (NCV), but NCV is affected by many factors, including temperature changes around the nerve, diameter of the axon, degree of myelinization etc. Ye et al. (2001) presumed that the tail club of *M. hochuanensis* not only worked as an efficient defense weapon, but also a sensitive sensory organ, which is supported by our FEA analyses.

4 Conclusions

To sum up, our FEA analyses indicate that as a defense weapon, the tail club of *Mamenchisaurus hochuanensis* is restricted by its size and the structure of the terminal caudal vertebrae, and thus the impacting function of the tail club would have been very limited. This result is different from previous views of the tail-club function in *M. hochuanensis* and here we support that of al. (2001) in seeing the coronal-tail club of ZDM 0126 as a true tail club. The tail club was more possible to work as a sensory organ to improve the NCV, enhancing the capacity of sensory perception towards the surroundings.

Acknowledgements

The authors thank Ji Qiang (Institute of Geology, Chinese Academy of Geological Sciences, China), Wu Xiaochun (Canadian Museum of Nature, Canada), Zhou Yuanming (Zigong Dinosaur Museum, China), and Liao Huijun (Beijing University of Aeronautics and Astronautics, China) for their critical comments and suggestions on this paper. Thanks to Wang Shenna and Zhu Wei for their kind help and assistance. This research was supported by the Chinese Ministry of Science and Technology (973 Project, 2006CB701405); China Geological Survey; National Natural Science Foundation of China; Accurate Reconstruction of Dinosaurs (Zigong Dinosaur Museum Project, 20071201); and the Palaeobiology Program of Chinese National Geography International (CNGi). ① Beijing University of Aeronautics and Astronautics provided software support for the study.

Note: **Institutional Abbreviations**: **AMNH**, American Museum of Natural History, New York, USA; **ROM**, Royal Ontario Museum, Toronto, Canada; **ZDM**, Zigong Dinosaur Museum, Sichuan Province, P. R. China.

Manuscript received Dec. 9, 2008
accepted May 26, 2009
edited by Susan Turner

References

Boyd, A., 2007. 2D and 3D retrodeformation techniques using finite element analysis with application to trilobites and *Herrerasaurus*. *Journal of Vertebrate Paleontology*, 27(3): 51A.

Buchholz, E.B., 1990. Gross spinal anatomy and limb use in living and fossil reptiles. *Paleobiology*, 16: 448–458.

Coombs, W.P.J., 1978. The families of the ornithischian dinosaur order Ankylosauria. *Palaeontology*, 21:143–170.

Coombs, W.P.J., 1995. Ankylosaurian tail clubs of middle Campanian to early Maastrichtian age from western North America, with description of a tiny club from Alberta and discussion of tail orientation and tail club function. *Canadian Journal of Earth Sciences*, 32(7): 902–912

Dong Zhiming, Peng Guangzhao and Huang Daxi, *1989.* The discovery of the bony tail club of sauropods. *Vertebrata PalAsiatica*, 27(3): 219–224 (in Chinese with English abstract).

Falkingham, P.L., Manning, P.L. and Margetts, L., 2007. Finite Element Analysis of dinosaur tracks. *Journal of Vertebrate Paleontology*, 27(3): 73A.

Fang Xiaosi, Zhao Xijin, Lu Liwu and Cheng Zhengwu, 2004. Discovery of Late Jurassic Mamenchisaurus in Yunnan, southwestern China. *Geological Bulletin of China*, 23(9–10): 1005–1011 (in Chinese with English abstract).

Fastnacht, M., Hess, N., Frey, E., and Weiser, H.P., 2002. Finite element analysis in vertebrate palaeontology. *Senckenbergiana Lethaea*, 82: 195–206.

Galton, P.M., and Upchurch, P., 2004. Stegosauria. In: Weishampel, D.B., Dodson, P., and Osmólska, H. (eds.), *The Dinosauria*, 2nd edn. Berkeley: University of California Press, 343–362.

Gilmore, C.W., 1936. Osteology of *Apatosaurus* with special reference to specimens in the Carnegie Museum. *Memoirs of the Carnegie Museum*, 11: 175–300

He Xinlu, Yang Suihua, Cai Kaiji, Li Kui and Liu Zongwen, 1996. A new species of sauropod, *Mamenchisaurus anyuensis* sp. nov. *Proceedings of the 30th International Geological Congress*, 12: 83–86 (in Chinese with English abstract).

Holland, W.J., 1906. Osteology of *Diplodocus* Marsh. *Memoirs of the Carnegie Museum*, 2: 225–278.

Holland, W.J., 1915. Heads and Tails: a few notes relating to the structure of sauropod dinosaurs. *Annals of the Carnegie Museum*, 9: 273–278.

Hou Lianhai, Zhou Shiwu and Cao Youshu, 1976. New discovery of sauropod dinosaurs from Sichuan. *Vertebrata PalAsiatica*, 14(3): 160–165 (in Chinese with English abstract).

Jenkins, I., 1997. Finite element analysis of skull dynamics in Permian synapsid (mammal-like-reptile) carnivores. *Journal of Morphology*, 232: 271.

Jenkins, I., Thomason, J.J., and Norman, D.B., 2002. Primates and engineering principles: applications to raniodental mechanisms in ancient terrestrial predators. *Senckenbergiana Lethaea*, 82: 223–240.

Komzsik, L., 2003. *The Lanczos method evolution and application*. Philadelphia: SIAM, 1–87.

Laura, B.P., 2007. Feeding and jaw mechanism in *Heterodontosaurus tucki* using Finite Element Analysis. *Journal of Vertebrate Paleontology*, 27(3): 131A.

Li Kui and Cai Kaiji, 1997. Classification and evolution of *Mamenchisaurus*. *Journal of Chengdu University of Technology*, 24: 102–107. (in Chinese)

Myhrvold, N.P., and Currie, P.J., 1997. Supersonic sauropods? Tail dynamics in the diplodocids. *Paleobiology*, 23: 393–409.

Ouyang Hui and Ye Yong, 2002. *The first mamenchisaurian skeleton with complete skull Mamenchisaurus youngi. Chengdu*. Sichuan Publishing House of Science and Technology, 1–111 (in Chinese with English summary)

Peng Guangzhao, Ye Yong, Gao Yuhui, Shu Chunkang and Jiang Shan., 2005. *Jurassic Dinosaur Faunas in Zigong*. Chengdu: Peoples Publishing House of Sichuan Province, 1–236. (in Chinese with English summary)

Pi Xiaozhong, Ouyang Hui and Ye Yong, 1996. A new species of sauropod from Zigong, Sichuan: *Mamenchisaurus youngi*. In: Department of Spatial Planning and Regional Economy (ed.). *Papers on Geoscience Contributed to the 30th International Geological Congress*. Beijing: China Economic Publishing House, 87–91 (in Chinese).

Rayfield, E.J., 1998. Finite element analysis of the snout of *Megalosaurus bucklandi*. *Journal of Vertebrate Paleontology*, 18, 71A

Rayfield, E.J., 2004. Cranial mechanics and feeding in *Tyrannosaurus rex*. *Proceedings of the Royal Society of London Series B-Biological Sciences*, 271: 1451–1459.

Rayfield, E.J., 2005a. Aspects of comparative cranial mechanics in the theropod dinosaurs *Coelophysis*, *Allosaurus* and *Tyrannosaurus*. *Zoological Journal of the Linnean Society* 144 (3): 309–316.

Rayfield, E.J., 2005b. Using finite-element analysis toinvestigate suture morphology: a case study using largecarnivorous dinosaurs. *The Anatomical Record*, 283A, 349–365.

Rayfield, E.J., 2007. Finite element analysis and understanding the biomechanics and evolution of living and fossil organisms. *Annual Review of Earth and Planetary Sciences*, 35: 541–576.

Rayfield, E.J., Norman, D B., Horner, C.C., Horner, J.R., May Smith, P., Thomason, J.J. and Upchurch, P., 2001. Cranial design and function in a large theropod dinosaur. *Nature*, 409: 1033–1037.

Rayfield, E.J., Norman, D.B. and Upchurch, P., 2002. Prey attack by a large theropod dinosaur: reply. *Nature*, 416, 388.

Russell, D.A. and Zheng, Z., 1993. A large mamenchisaurid from the Junggar Basin, Xinjiang, People's Republic of China. *Canadian Journal of Earth Sciences*, 30(10 and 11): 2082–2095.

Snively, E. and Russell, A. 2002. The tyrannosaurid metatarsus: bone strain and inferred ligament function. *Senckenbergiana Lethaea*, 82: 35–42

Thomason, J.J., 1995. To what extent can the mechanical environment of a bone be inferred from its architecture? In: Thomason, J.J. (ed.), *Functional morphology in vertebrate paleontology*. Cambridge: Cambridge University Press. 249–263

Vickaryous, M.K., Maryanska, T., and Weishampel, D.B., 2004. Ankylosauria. In: Weishampel, D.B., Dodson, P., and Osmólska, H. (eds.). *The Dinosauria*. 2nd edition. Berkeley: University of California Press, 363–392.

Wilson, J.A., Martinez, R.N., and Alcober, O., 1999. Distal tail segment of a titanosaur (Dinosauria: Sauropoda) from the Upper Cretaceous of Mendoza, Argentina. *Journal of Vertebrate Paleontology*, 19: 591–594.

Witzel, U., and Preuschoft, H., 2005. Finite-element model construction for the virtual synthesis of the skulls in vertebrates: case study of *Diplodocus*. A*natomical Record*, 238A: 391–401.

Ye Yong, Ouyang Hui and Fu Qianming, 2001. New material of *Mamenchisaurus hochuanensis* from Zigong, China. *Vertebrata PalAsiatica*, 39(4): 266–271 (in Chinese with English abstract).

You Hailu, Tang Feng and Luo Zhexi, 2003. A new basal titanosaur (Dinosauria: Sauropoda) from the Early Cretaceous of China. *Acta Geologica Sinica* (English Edition), 77(4): 424–429.

Young (Yang), C.C(Z.j), 1954. On a new sauropod from Yiping, Szechuan, China. *Scientia Sinica*, 3(4): 481–504 (in Chinese with English abstract).

Young(Yang), C.C(Z.j),, and Chao(Zhao), X.J(X.j)., 1972. *Mamenchisaurus hochuanensis* sp. nov. Institute of Vertebrate Paleontology and Paleoanthropology, *Monograph* (ser. A), 8: 1–30 (in Chinese with English abstract)

Zhang Yihong, Yang Daihuan and Peng Guangzhao, 1984. New materials of *Shunosaurus* from the Middle Jurassic of Dashanpu, Zigong, Sichuan. *Journal of the Chengdu College of Geology* 2, (Suppl.): 1–12 (in Chinese).

Zhang Yihong, Li Kui and Zeng Qinghua, 1998. A new species of sauropod dinosaur from the Upper Jurassic of Sichuan Basin, China. *Journal of Chengdu University of Technology*, 25(1): 61–70 (in Chinese).